RSC Advances

PAPER

View Article Online
View Journal | View Issue

Cite this: *RSC Adv.*, 2021, **11**, 32038

Fabrication of a superhydrophobic surface by straightforward immersion for copperplate artwork protection

Jingming Liu,[a] Min Wang,[b] Chengyu Gu,[b] Lehua Zhang[b] and Ying Yan*[b]

With the background of contemporary art, using comprehensive materials to create artworks is becoming more and more common. The new era of digital image-based copperplate artworks, using photosensitive lithography, has given traditional art forms new life and greater popularity in the digital age. However, the patterns and textures of the works created by the new techniques are generally shallow, and the copper surface is easily damaged and loses its aesthetic value, which makes it a practical problem to protect such works more effectively. In this paper, a facile method is adopted, wherein a superhydrophobic film is constructed on the surface of copperplate images by straightforward immersion in (heptadecafluoro-1,1,2,2-tetradecyl)trimethoxysilane (FAS-17) solution to achieve the anticorrosive protection of copperplate artworks. The hydrophobicity of the copper surface was analyzed using an instrument that measures contact angles. The superhydrophobic surface morphology and composition were analyzed with a scanning electron microscope coupled with an energy-dispersive spectrometer, and the corrosion resistance was analyzed using an electrochemical workstation. A systematic study is presented on the effect of the immersion time in FAS-17 and the concentration of FAS-17, and the optimal preparation conditions of the superhydrophobic film were determined, which means that the copper substrates were immersed in 0.7 mol L^{-1} FAS-17 for 40 min. After the treatment of the surface to make it superhydrophobic, the contact angle and the corrosion inhibition efficiency of the copperplate etching surface reached 161.2° and 95.7%, respectively. The results show that the superhydrophobic film was successfully prepared on the surface of the artwork based on copper, which can effectively improve the corrosion resistance and is beneficial for the long-term protection of artwork.

Received 2nd October 2020
Accepted 9th September 2021

DOI: 10.1039/d0ra08233c

rsc.li/rsc-advances

1. Introduction

Copperplate artworks are also known as copperplate etchings and copperplate paintings. The art of etching is elegant and has been regarded as a rare type of painting. All the masters of past artistic dynasties were deeply focused on the artistic creation of etchings. From the German Durer to the Dutch Rembrandt, from the Spanish Goya to the French impressionists Manet, Monet, Sislan, Degas, and so on, to the modern Picasso and Matisse, artistic masters have left very exquisite etchings. There are many production methods but anticorrosive wax or preservatives (generally made of yellow wax, rosin, asphalt and other acid-resistant materials) are usually used in a coating layout, forming a layer of anticorrosive film. A needle is used for the layout painting and then the image is placed in the corrosive solution (commonly a nitric acid solution). The point at which the needle scratches off the anticorrosive film, that is, where corrosion takes place, a concave line is formed, and the longer the corrosion time, the deeper the concave line after removing the anticorrosive film; this plate is then used on the copperplate machine for gravure printing. Due to the line thickness, depth, and density, the printed works will form a multi-level, complex picture with tonal change.

The art of copper etchings enjoys a worldwide reputation for its advanced technology and cultural connotations over the years, which make it quite precious. In contemporary times, copper etchings appear as new and creative methods and have become a new artistic carrier. Combined with the traditional art of new media and digital technology, the ancient etchings form the digital image-based etchings of the new era. Etchings based on digital images are not the same as traditional techniques; they are no longer in the form of direct hand painting but computers are first used for image creation, then the satisfactory image is output into a film, using the film to expose the copper plate coated with photosensitive adhesive or film to obtain the digital copperplate artwork. Although these artworks created with this new technique have strong availability and popularity, there are also some shortcomings. For example, the patterns and textures formed are generally shallow, and beauty

[a]*Shanghai Academy of Fine Arts, Shanghai University, Shanghai 200444, China*
[b]*State Environmental Protection Key Laboratory of Environmental Risk Assessment and Control on Chemical Process, East China University of Science and Technology, Shanghai 200237, China. E-mail: wendy0101@126.com*

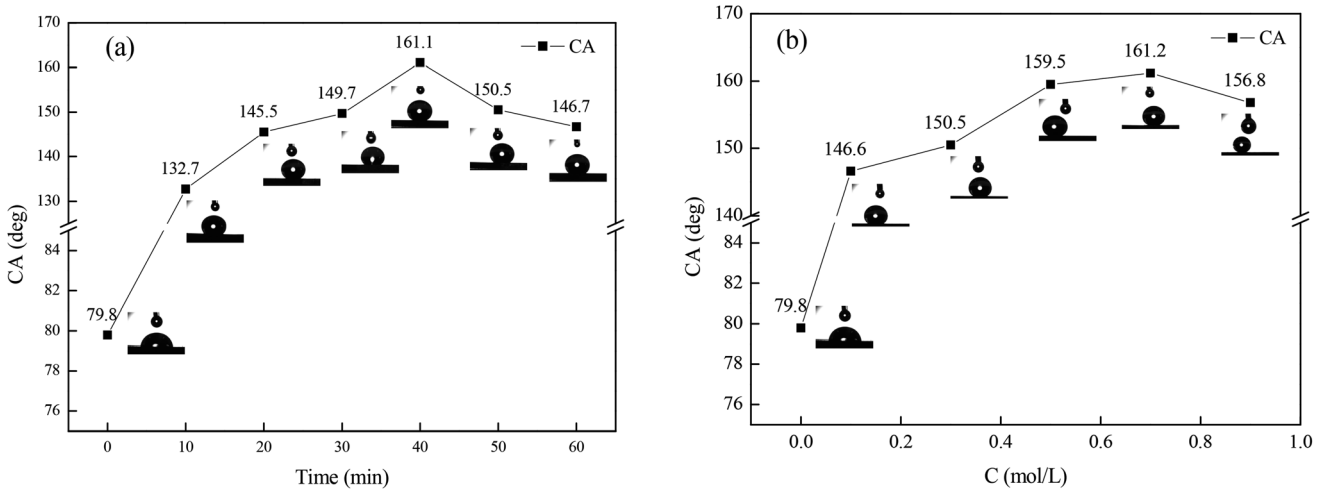

Fig. 1 The water contact angles of the samples. (a) The effect of the immersion time with the FAS-17 concentration of 0.5 mol L^{-1} at 298 K. (b) The effect of the concentration of FAS-17 when the immersion time was 40 min.

and value are easily lost because the copper surface is corroded. How to more effectively protect copper bases from corrosion is a practical problem for the long-term preservation of such artworks.

Although copper and its alloys are characterized by relatively good corrosion resistance and fouling resistance, they are prone to corrosion and serious surface discoloration due to long-term exposure to humid air or the presence of corrosive media such as CN^- and Cl^-.[1] Corrosion inhibition is one of the effective methods for solving the problem of the corrosion of copper and its alloys. At present, the most extensive method is to select suitable organic compounds as corrosion inhibitors, such as benzotriazole and its derivatives, various thiazole derivatives[2] and imidazole.[3] However, most of these inhibitors are expensive and toxic and are not good for the environment, so their use is limited. As such, the development of an environmentally friendly and economical metal protective layer on copper surfaces has gradually become a research hotspot in recent years. The superhydrophobic surface method has been attracting more and more attention[2] and it is based on the concept of "the Lotus effect" proposed by German botanist Wilhelm Barthlott.[1,4] The superhydrophobic surface method that mimics

Table 1 f_1 and f_2 values of samples with different immersion times

Immersion time	f_1	f_2
Blank	1.000	0.000
10 min	0.273	0.726
20 min	0.149	0.850
30 min	0.116	0.883
40 min	0.046	0.953
50 min	0.110	0.889
60 min	0.139	0.860

Table 2 f_1 and f_2 values of samples immersed in different concentration of FAS-17

Concentration (mol L^{-1})	f_1	f_2
Blank	1.000	0.000
0.1	0.140	0.859
0.3	0.064	0.935
0.5	0.031	0.968
0.7	0.026	0.973
0.9	0.040	0.959

Fig. 2 Anti-corrosion effect of copperplate digital images with a superhydrophobic surface. (a) Image with a superhydrophobic surface; (b) image without a superhydrophobic surface; (c) image with a superhydrophobic film tested in an ozone aging chamber for 7 days; (d) image without a superhydrophobic film tested in an ozone aging chamber for 7 days.

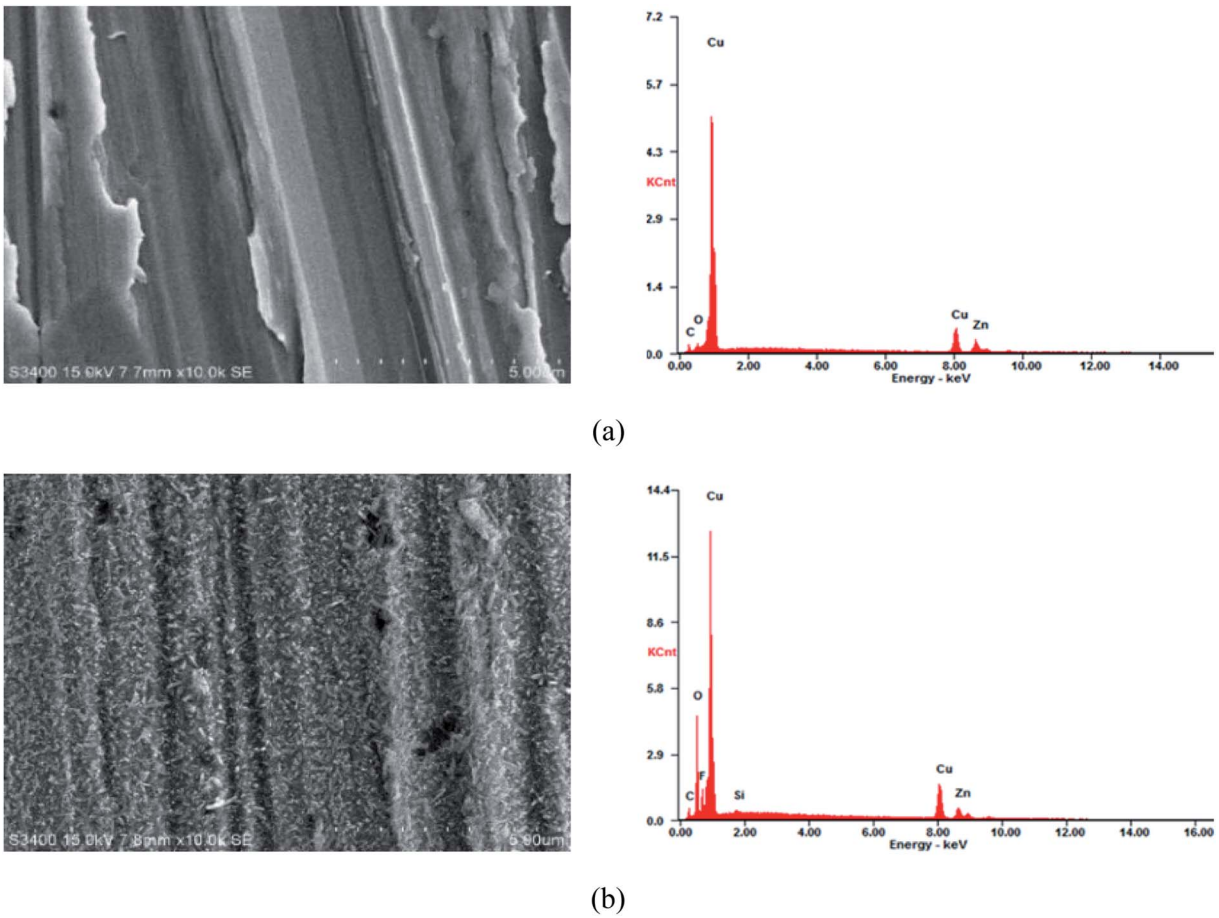

Fig. 3 SEM-EDS image of a copper specimen surface. (a) Surface of a copper substrate; (b) surface of a copper substrate with superhydrophobic film.

the lotus leaf effect has the advantages of hydrophobicity and self-cleaning.[2–6]

At present, the preparation of a superhydrophobic surface can be roughly divided into two categories: the construction of a micron-nano-sized rough structure on the surface of hydrophobic materials with low surface energy or modifications of this rough structure using low-surface energy materials.[7] Preparation methods for superhydrophobic surfaces mainly include the template method, the electrochemical method, the etching method,[8] the gel method,[9] the layered self-assembly method[10] and so on. Active hydrophobic organic molecular groups used to prepare superhydrophobic films on the surface of metal bases include –SiOH, –SH, and –COOH.[9] Common hydrophobic materials include siloxane, fluoroalkyl silane, nutmeg acid, stearic acid,[11,12] *etc.*

The study of superhydrophobic surfaces has generally focused on pure metal or alloys. Recently, the fabrication of superhydrophobic surfaces has been applied to the surfaces of pure copper,[13] magnesium alloy[14] and other metals. Due to the special structural composition of copperplate artistic works, many difficulties remain in the study of superhydrophobic surfaces. At present, there are few studies in this field.

In this paper, a (heptadecafluoro-1,1,2,2-tetradecyl) trimethoxysilane (FAS-17) solution was used to prepare a superhydrophobic surface on copperplate artworks. The hydrophobicity and corrosion resistance of superhydrophobic surfaces have been investigated. By measuring contact angles, surface hydrophobicity was analyzed, and the superhydrophobic surface morphology characteristics and composition analysis were determined using a scanning electron microscope coupled with an energy-dispersive spectrometer. An electrochemical workstation was used to perform the corrosion resistance analysis to prove that this method has a good inhibitory effect on copper corrosion. This study can be used as a reference for long-term anti-corrosion protection of copperplate artworks by preparing long-acting and durable superhydrophobic anti-corrosion surfaces and enhancing the cleanliness and aesthetics of the works' surfaces.

2. Materials and methods

The materials used in the study were from a copperplate etching, whose components were Cu ≥ 58.34%, Zn ≥ 38.63%, and C ≤ 2.11%. The superhydrophobic reagent was FAS-17 (≥99.8%, AR, Tokyo Chemical Industry Co. Ltd). The reagents used in the ultrasonic cleaning were anhydrous ethanol (≥99.7%, AR, Shanghai Titan Technology Co. Ltd) and acetone (≥99.5%, AR, Sinopharm Group Chemical Reagent Co. Ltd).

Table 3 Elemental compositions of the copper substrate plate and the copper substrate plate with super-hydrophobic film

Elemental compositions	Cu/wt%	Zn/wt%	C/wt%	O/wt%	F/wt%	Si/wt%
Blank	58.34	38.63	2.11	0.93	—	—
Copper substrate with superhydrophobic film	59.55	24.37	2.32	11.00	2.28	0.49

The copperplate etching of size 10 mm × 10 mm × 1 mm was polished using 400-1500# abrasive paper and then cleaned with acetone, ethanol, and deionized water for 10 min. The pretreated copper samples were immersed in the mixture of sodium hydroxide with a concentration of 2.50 mol L^{-1} and ammonium persulphate with a concentration of 0.23 mol L^{-1} for 15 min to obtain a rougher surface structure, and then cleaned and dried. After immersing in different concentrations of FAS-17 for a certain time, the test pieces were taken out of the solution, washed with ethanol several times, and dried naturally in the air.

The copperplate artworks that were dipped and not dipped were placed in an ozone aging chamber at 30 °C for the corrosion test. The test lasted 7 days and included an ozone concentration of 100 ppm and a humidity of 85%.

A GonloStar200 contact angle measuring instrument was used to measure the contact angle of the sample surface at room temperature. The liquid droplet volume was 14 μL. The superhydrophobic surface morphology was observed using an S-3400 scanning electron microscope coupled with energy-dispersive spectroscopy (SEM-EDS).

The electrochemical impedance spectra (EIS) and the polarization curves (Tafel) were obtained on a CHI600E electrochemical workstation. A standard three-electrode system was adopted. The exposed area of the working electrode was 1.0 cm^2, the platinum wire electrode was used as the auxiliary electrode, and the calomel electrode was used as the reference electrode.

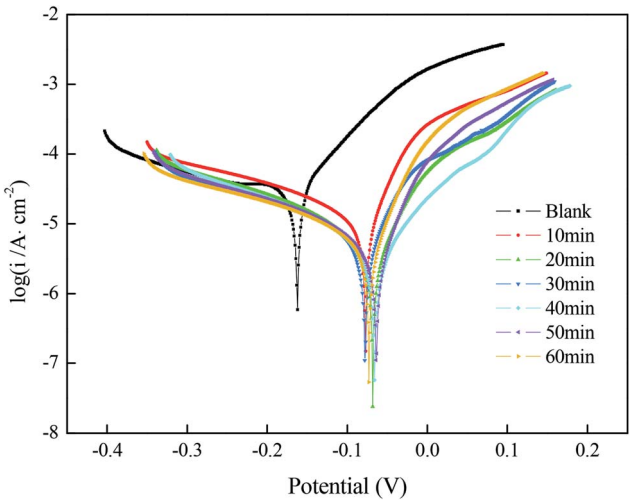

Fig. 4 Polarization curves of a copper substrate with super-hydrophobic film prepared under different immersion times in a solution simulating atmospheric conditions.

The corrosive medium was a solution that simulated atmospheric conditions, which contained 0.028 mol L^{-1} NaCl + 0.01 mol L^{-1} Na_2SO_4 + 0.016 mol L^{-1} $NaHCO_3$. The working electrode was immersed in this solution for 2 h in advance and tested at room temperature after the open circuit potential was stable. The EIS scanning range was 10 mHz to 95 kHz, and the ac amplitude was 10 mV. The scanning range of the polarization curve was ±250 mV (relative to the open circuit potential), and the scanning rate was 1 mV s^{-1}.

3. Results and discussion

3.1 Contact angle measurement

In order to determine the optimal immersion time and concentration of FAS-17 for obtaining the copperplate artworks with the best superhydrophobicity, experiments were conducted based on the single-factor method, which is shown as Fig. 1. FAS-17 plays an important role in the change of the copper surface wettability. For the bare copperplate artwork, the water droplets were semi-circular on the surface and the contact angle was 79.8°. As shown in Fig. 1(a), when immersion time was increased to 40 min, the contact angle between the surface and the water of the test piece superhydrophobic film reached the maximum value of 161.1°. Fig. 1(b) shows that the CA reached the maximum value of 161.2° with the concentration of FAS-17 of 0.7 mol L^{-1}. With further increase in the immersion time and the concentration of FAS-17, the CA of the copper surface decreased, which can be explained by the damage to the superhydrophobic film. Thus, the optimal preparation process of the superhydrophobic film was immersion in FAS-17 with a concentration of 0.7 mol L^{-1} for 40 min.

The superhydrophobicity can be expressed by the Cassie–Baxter equation (eqn (1)):[15]

$$\cos\theta_c = f_1 \cos\theta - f_2 \quad (1)$$

Table 4 Electrochemical parameters of the polarization curve of specimens in a solution simulating atmospheric conditions

Immersion time	E_{corr}/mV	J_{corr}/mA cm^{-2}	βa/mV	βc/mV	η/%
0 min	−0.162	5.70×10^{-2}	489.00	75.57	—
10 min	−0.077	3.28×10^{-2}	236.29	54.74	42.5
20 min	−0.068	8.47×10^{-3}	190.08	68.90	85.1
30 min	−0.078	1.24×10^{-2}	240.67	70.97	78.2
40 min	−0.062	5.07×10^{-3}	191.46	70.35	91.1
50 min	−0.066	7.98×10^{-3}	208.68	56.08	86.0
60 min	−0.068	1.03×10^{-2}	230.63	51.88	81.9

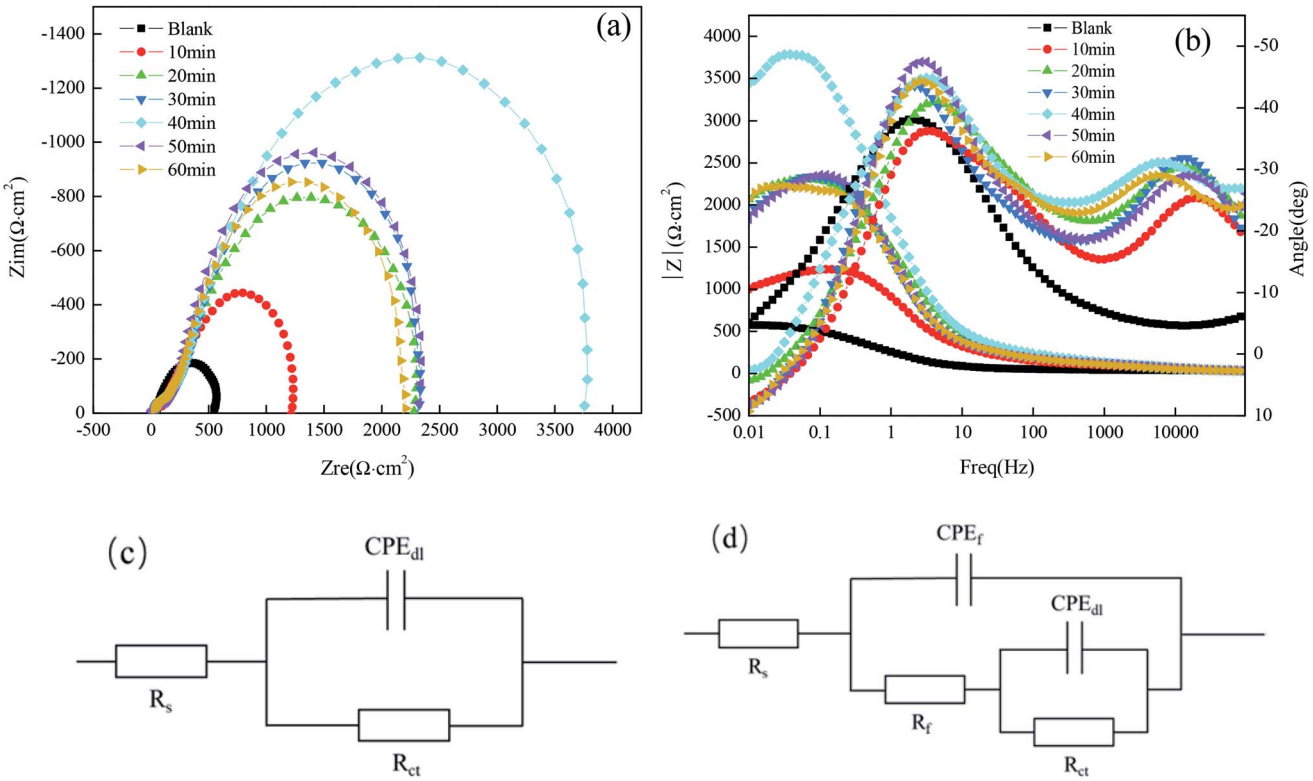

Fig. 5 Nyquist (a) plots and Bode (b) plots of the copper substrate before and after the fabrication of the superhydrophobic surface by immersion in the solution simulating atmospheric conditions; (c) the equivalent circuit used for the copper substrate; (d) the equivalent circuit used for the copper substrate after superhydrophobic surface formation.

where θ_c and θ refer to the water contact angles of the copper substrate modified by FAS-17 and the bare copper substrate, respectively. f_1 and f_2 are the area fractions of liquid with solid and air, respectively ($f_1 + f_2 = 1$). The calculated values of f_1 and f_2 are given in Tables 1 and 2.

f_2 reached the maximum values of 95.3% and 97.3% under the optimal conditions, which indicated that the "air cushion" hinders the direct contact of water droplets with the copperplate artwork.[16]

3.2 Superhydrophobic surface protection of copperplate etchings

Fig. 2 shows an effect diagram for the superhydrophobic surface anti-corrosion effects of copperplate artworks. The comparison of Fig. 2(a) and (b) shows that the appearance of the copperplate artworks does not change significantly after dipping and coating in the superhydrophobic protective film; *i.e.*, the film does not affect the aesthetic value. The comparison of Fig. 2(a) and (c) shows that the corrosion of the copperplate artworks is not obvious after 7 days in an ozone aging chamber, due to the superhydrophobic protective film. Fig. 2(a) and (d) show that the corrosion of the copperplate artistic work without superhydrophobic protective film was evidenced after 7 days in the ozone aging chamber. Fig. 2(c) and (d) show that the dip-coating had an obvious protective effect on the corrosion of the copperplate artwork.

3.3 Morphology characteristics and surface composition analysis of the superhydrophobic surface

Fig. 3 shows the scanning electron microscope image of the copperplate specimen without and with the superhydrophobic

Table 5 Electrochemical impedance parameters obtained from EIS fitting under different immersion times

Immersion time	R_s/Ω cm^2	Y_{CPEf}/Ω^{-1} cm^{-2}	n_f	R_f/Ω cm^2	Y_{CPEdl}/Ω^{-1} cm^{-2}	n_{dl}	R_{ct}/Ω cm^2
0 min	36.13	—	—	—	0.001106	0.6263	609.6
10 min	20.28	2.156×10^{-5}	0.5981	106.8	1.603×10^{-4}	0.7285	1147
20 min	20.36	2.402×10^{-5}	0.5667	214.8	1.413×10^{-4}	0.6426	1982
30 min	19.41	2.679×10^{-5}	0.5783	218.3	1.119×10^{-4}	0.8211	2190
40 min	17.54	4.496×10^{-5}	0.5493	272.1	7.536×10^{-5}	0.7871	3813
50 min	18.51	6.135×10^{-5}	0.4131	204.0	8.036×10^{-5}	0.8679	2331
60 min	19.01	5.003×10^{-5}	0.5657	204.5	9.260×10^{-5}	0.8250	2169

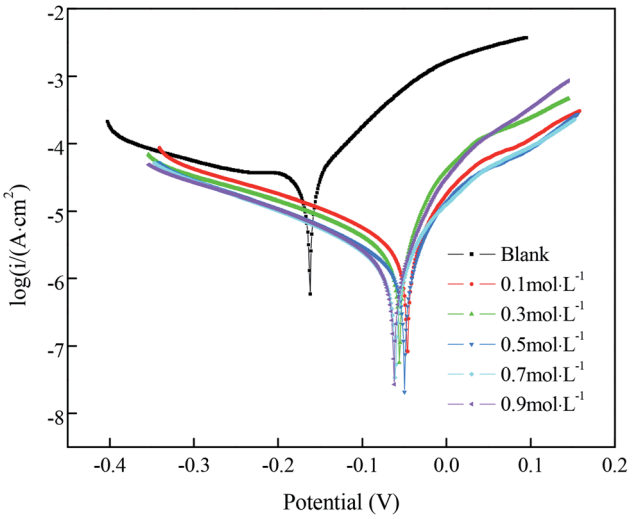

Fig. 6 Polarization curves of a copper substrate under different concentrations of FAS-17 in solutions simulating atmospheric conditions.

Table 6 Electrochemical parameters of the polarization curve of specimens in solutions simulating atmospheric conditions

Concentration	E_{corr}/mV	J_{corr}/mA cm^{-2}	βa/mV	βc/mV	η/%
0 mol L^{-1}	−0.162	5.70×10^{-2}	489.00	75.57	—
0.1 mol L^{-1}	−0.049	6.79×10^{-3}	189.79	63.33	88.1
0.3 mol L^{-1}	−0.061	5.85×10^{-3}	193.54	47.54	89.7
0.5 mol L^{-1}	−0.057	3.56×10^{-3}	172.47	56.61	93.8
0.7 mol L^{-1}	−0.051	2.46×10^{-3}	171.94	70.88	95.7
0.9 mol L^{-1}	−0.065	2.95×10^{-3}	173.07	52.05	94.8

film. There were some scratches on the surface of the test piece of the copper substrate (Fig. 3(a)), and the substrate surface was relatively smooth between scratches. The surface morphology with the superhydrophobic film is shown in Fig. 3(b), which was covered with a dense network structure. This microstructure produced numerous holes to trap air and increased gas–liquid contact area, so that corrosion inhibition performance was improved. According to the EDS data (Table 3), carbon, oxygen and silicon contents increased after superhydrophobic treatment, indicating that a superhydrophobic film was formed on the surface of the test piece.

3.4 Electrochemical impedance characteristics and corrosion resistance of copper with superhydrophobic surfaces

3.4.1 Effect of immersion time. Fig. 4 shows the polarization curve of the copper substrate test sample with superhydrophobic film prepared under different immersion times in a solution simulating atmospheric conditions. The fitting results are shown in Table 4. E_{corr} is the self-corrosion potential. η is the corrosion inhibition efficiency and it is calculated as the following relationship:[17]

$$\eta = (1 - J_{corr}/J^0_{corr}) \times 100\%$$

where, J^0_{corr} and J_{corr} are the self-corrosion current densities of the copper substrate test plates before and after superhydrophobic treatment, respectively. The corrosion potentials of the copper substrate all changed and had a lower corrosion current density after the fabrication of the superhydrophobic surface. It can be seen from Table 4 that E_{corr} reached the maximum value of −0.062 mV and J_{corr} reached the minimum value of 5.07×10^{-3} mA cm^{-2} when the immersion time was 40 min. According to the calculations, η reached 91.1%, indicating that the superhydrophobic film formed on the test plate surface could effectively prevent the plasma diffusion of Cl^-, HCO_3^-, CO_3^{2-} and S^{2-} from the solution to its surface and improve the corrosion resistance of the test plate.

Fig. 5(a) shows the Nyquist plots and their fitting for the copper substrate samples before and after fabrication of the superhydrophobic surface by immersion in a solution simulating atmospheric conditions. The arc diameter of the

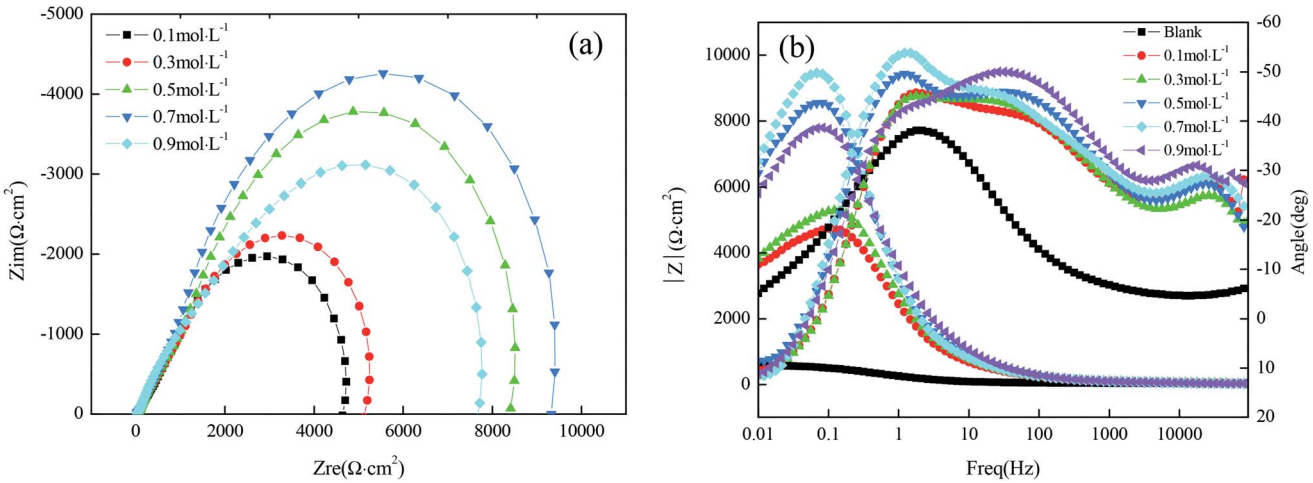

Fig. 7 Nyquist (a) plots and Bode (b) plots of the copper substrate in solutions simulating atmospheric conditions.

Table 7 Electrochemical impedance parameters obtained from EIS fitting under different concentrations of FAS-17

Concentration	R_s/Ω cm^2	Y_{CPEf}/Ω^{-1} cm^{-2}	n_f	R_f/Ω cm^2	Y_{CPEdl}/Ω^{-1} cm^{-2}	n_{dl}	R_{ct}/Ω cm^2
0 mol L^{-1}	36.13	—	—	—	0.001106	0.6263	609.6
0.1 mol L^{-1}	16.87	1.449×10^{-5}	0.6521	79.35	6.788×10^{-5}	0.6801	5.020×10^3
0.3 mol L^{-1}	17.92	1.687×10^{-5}	0.5594	80.73	6.165×10^{-5}	0.6657	5.793×10^3
0.5 mol L^{-1}	19.52	2.679×10^{-5}	0.5783	82.67	5.735×10^{-5}	0.6651	2.190×10^3
0.7 mol L^{-1}	18.28	1.376×10^{-5}	0.6616	112.2	5.386×10^{-5}	0.7021	1.063×10^4
0.9 mol L^{-1}	13.24	1.691×10^{-5}	0.6907	75.83	5.607×10^{-5}	0.6728	8.271×10^3

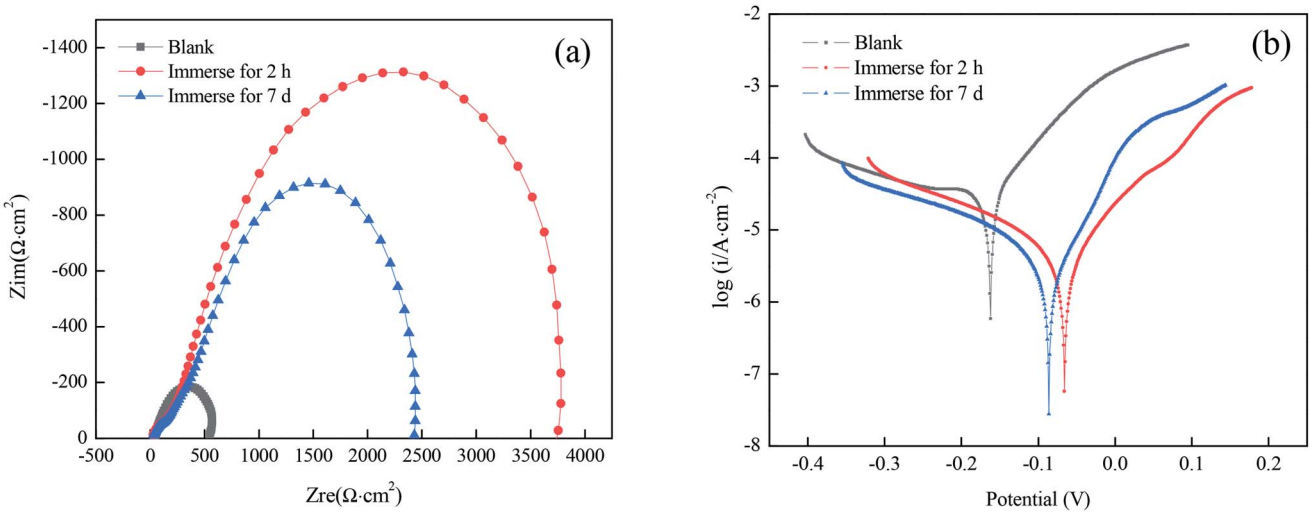

Fig. 8 Nyquist plots (a) and polarization curves (b) for superhydrophobic copper in a solution simulating atmospheric conditions for different immersion times.

capacitive reactance first increased and then decreased with the increasing immersion time. It is worth mentioning that the larger arc diameter represents higher charge transfer resistance.[18] As shown in Fig. 5(a), when the immersion time was 40 min, the arc radius of the superhydrophobic sample was the largest, which is consistent with the results of the polarization curves.

It can be seen from Fig. 5(b) that there is one time constant for the untreated copper substrate and there are two time constants for the superhydrophobic specimens, so the measured results can be fitted by the electrical equivalent circuit shown in Fig. 5(c) and (d), respectively. The fitted EIS parameters are listed in Table 5.

Table 5 shows that the R_{ct} (the charge transfer resistance) tended to increase, especially for the immersion time of 40 min, reaching 3813 Ω cm^2, which increased by one order of magnitude as compared to the bare copper. The larger the charge transfer resistance, the more difficult it is for the corrosion medium to transfer to the copper surface and to produce an electrochemical corrosion reaction. The R_f (the surface film resistance) had a similar tendency to the R_{ct}. The changes in the values of R_{ct} and R_f indicate that the corrosion resistance of the copper substrate surface after the fabrication of the superhydrophobic surface with FAS-17 was significantly improved.

3.4.2 The effect of FAS-17 concentration. Fig. 6 shows the polarization curve of bare copper and superhydrophobic copper surfaces under five different concentrations of FAS-17. The electrochemical parameters obtained from the Tafel curves are given in Table 6. It can be seen that all of the superhydrophobic samples have a lower corrosion current density as compared to bare copper. When the concentration of FAS-17 was 0.7 mol L^{-1}, the corrosion current density achieved the minimum value of 2.46×10^{-3} mA cm^{-2} and the corrosion inhibition efficiency reached 95.7%, indicating that the corrosion rate of the copper

Table 8 EIS fitting results of superhydrophobic copper in a solution simulating atmospheric conditions for different immersion times

Time	R_s/Ω cm^2	Y_{CPEf}/Ω^{-1} cm^{-2}	n_f	R_f/Ω cm^2	Y_{CPEdl}/Ω^{-1} cm^{-2}	n_{dl}	R_{ct}/Ω cm^2
Blank	36.13	—	—	—	0.001106	0.6263	6.096×10^2
Immerse for 2 h	17.54	4.496×10^{-5}	0.5493	272.1	7.536×10^{-5}	0.7871	3.813×10^3
Immerse for 7 d	18.24	4.691×10^{-5}	0.6907	156.83	8.407×10^{-5}	0.6728	2.371×10^3

Table 9 Electrochemical parameters of superhydrophobic copper in a solution simulating atmospheric conditions for different immersion times

Time	E_{corr}/V	I_{corr}/mA cm^{-2}	βa/mV	βc/mV	η/%
Blank	−0.162	5.70×10^{-2}	489.00	75.57	—
Immerse for 2 h	−0.066	5.07×10^{-3}	191.46	70.35	91.1
Immerse for 7 d	−0.086	6.21×10^{-3}	208.33	102.93	89.1

substrate was the lowest at this time, which is consistent with the contact angle test result.

The Nyquist plots for samples immersed in different concentrations of FAS-17 are shown in Fig. 7(a). The sample with 0.7 mol L^{-1} FAS-17 treatment exhibited the largest diameter of capacitive loop, indicating that the copper substrate plate had the best superhydrophobicity under these conditions. Fig. 7(b) represents the Bode plots of the samples. There are two time constants for superhydrophobic samples, so Fig. 5(d) can be used to fit the electrochemical data; the results are listed in Table 7. Compared to the bare copper, both R_{ct} and R_f increased and peaked at about 1.063×10^4 Ω cm^2 and 112.2 Ω cm^2, respectively, at 0.7 mol L^{-1} of FAS-17. Combining Tables 5 and 7, it can be seen that the best process for preparing superhydrophobic films on the copper surface is to immerse in a FAS-17 solution with the concentration of 0.7 mol L^{-1} for 40 min.

3.5 Stability of the superhydrophobic film

To study the stability performance of superhydrophobic films prepared under optimal conditions, the impedance spectrogram and the polarization curves were obtained after immersion for 7 d in a solution simulating atmospheric conditions. As shown in Fig. 8(a), there was still a capacity loop in the high-frequency area after immersion for 7 d. Although the arc diameter was slightly smaller than that after immersion for 2 h, it was much larger than that of the bare copper substrate. According to Tables 8 and 9, the superhydrophobic film still had a good corrosion-inhibiting performance after immersion for 7 d, suggesting that the prepared superhydrophobic film has good stability.

4. Conclusion

A straightforward immersion method was adopted to prepare a superhydrophobic surface on copper by using a mixed solution of NaOH and $(NH_4)_2S_2O_8$ as a surface roughening reagent, and FAS-17 as a low surface energy modifier. The effects of the time of immersion in FAS-17 and the initial concentration of FAS-17 were studied and the results showed that the copper surface had the best superhydrophobicity on immersion in 0.7 mol L^{-1} FAS-17 for 40 min. Under the optimal conditions, both the contact angle and the corrosion inhibition efficiency reached the maximum value of 161.2° and 95.7%, respectively. Moreover, the stability performance of the superhydrophobic surface on the copper substrate was studied by electrochemical tests, and the results indicated that the superhydrophobic film had good stability. The superhydrophobic film was successfully built on the surface of the copper substrate by using FAS-17, and it can effectively improve the copper's corrosion resistance, which holds promising application prospects in the protection of copper-based artworks.

Conflicts of interest

There are no conflicts to declare.

References

1 S. Nishimoto and B. Bhushan, Bioinspired self-cleaning surfaces with superhydrophobicity, and superhydrophilicity, *RSC Adv.*, 2013, **3**, 671–690.
2 C. Y. Cao and J. Cheng, Fabrication of superhydrophobic copper stearate@Fe_3O_4 coating on stainless steel meshes by dip-coating for oil/water separation, *Surf. Coat. Technol.*, 2018, **349**, 296–302.
3 M. Ferrari and A. Benedetti, Superhydrophobic surfaces for applications in seawater, *Adv. Colloid Interface Sci.*, 2015, **222**, 291–304.
4 P. Wang, D. Zhang and R. Qiu, Green approach to fabrication of a super-hydrophobic film on copper and the consequent corrosion resistance, *Corros. Sci.*, 2014, **80**, 366–373.
5 L. K. Wu, X. F. Zhang and J. M. Hu, Corrosion protection of mild steel by one-step electrodeposition of superhydrophobic silica film, *Corros. Sci.*, 2014, **85**, 482–487.
6 Y. W. Zeng, Z. L. Qin, Q. H. Hua, *et al.*, Sheet-like superhydrophobic surfaces fabricated on copper as a barrier to corrosion in a simulated marine system, *Surf. Coat. Technol.*, 2019, **362**, 62–71.
7 C. C. Li, R. N. Ma, A. Du, *et al.*, One-step fabrication of bionic superhydrophobic coating on galvanised steel with excellent corrosion resistance, *J. Alloys Compd.*, 2019, **786**, 272–283.
8 H. Jie, Q. Xu, L. Wei, *et al.*, Etching and heating treatment combined approach for superhydrophobic surface on brass substrates and the consequent corrosion resistance, *Corros. Sci.*, 2016, **102**, 251–258.
9 Y. Gao, Y. Sun and D. Guo, Facile fabrication of superhydrophobic surfaces with low roughness on Ti–6Al–4V substrates via anodization, *Appl. Surf. Sci.*, 2014, **314**, 754–759.
10 Z. Duan, Z. Zhao, D. Luo, *et al.*, A facial approach combining photosensitive sol–gel with self-assembly method to fabricate superhydrophobic TiO_2 films with patterned surface structure, *Appl. Surf. Sci.*, 2016, **360**, 1030–1035.
11 Z. Yang, X. P. Liu and Y. L. Tian, Hybrid laser ablation and chemical modification for fast fabrication of bio-inspired super-hydrophobic surface with excellent self-cleaning, stability and corrosion resistance, *J. Bionic Eng.*, 2019, **16**, 13–26.
12 F. Y. Wang and Z. G. Guo, Facile synthesis of superhydrophobic three-metal-component layered double hydroxide films on aluminum foils for highly improved corrosion inhibition, *New J. Chem.*, 2019, **43**, 2289–2298.

13 L. X. Ma, L. N. Wang, C. Y. Li, *et al.*, Hybrid nanosecond laser processing and heat treatment for rapid preparation of super-hydrophobic copper surface, *Metals*, 2019, **9**, 668–676.
14 Z. W. Song, Z. H. Xie, L. F. Ding, *et al.*, Corrosion Resistance of Super-Hydrophobic Coating on AZ31B Mg Alloy, *Int. J. Electrochem. Sci.*, 2018, **13**, 6190–6200.
15 P. Sareh and N. Reza, A facile solution-immersion process for the fabrication of superhydrophobic gibbsite films with a binary micro-nano structure: effective factors optimization via Taguchi method, *Appl. Surf. Sci.*, 2015, **356**, 157–166.
16 E. Y. Liu, X. L. Yin, J. H. Hu, *et al.*, Fabrication of a biomimetic hierarchical superhydrophobic Cu-Ni coating with self-cleaning and anti-corrosion properties, *Colloids Surf., A*, 2020, **586**, 124223.
17 H. R. Wang and M. Y. Li, Preparation and Corrosion Inhibition of GPTMS/PFDS Self-Assembled Bilayer on 430 Stainless Steel, *Corros. Prot.*, 2014, **35**, 60–63.
18 T. T. Liang, H. Y. Yuan, C. C. Li, *et al.*, Corrosion inhibition effect of nano–SiO_2 for galvanized steel superhydrophobic surface, *Surf. Coat. Technol.*, 2021, **406**, 126673.